PCCP

Unveiling the MolecularStructure and Two-photon Absorption Properties Relationship of Branched Oligofluorenes

Journal:	*Physical Chemistry Chemical Physics*
Manuscript ID	CP-ART-11-2022-005189.R2
Article Type:	Paper
Date Submitted by the Author:	07-Dec-2022
Complete List of Authors:	Zucolotto Cocca, Leandro Henrique; Universidade de Sao Paulo Instituto de Fisica de Sao Carlos Pelosi, André; Instituto de Física de São Carlos - Universidade de São Paulo, Física e Ciência dos Materiais Abegão, Luis; Instituto de Física, Universidade Federal de Goiás, Physics - Photonics Group Garcia, Rafael; Universidade de São Paulo Instituto de Física de São Carlos Mulatier, Jean-Christophe; Ecole Normale Supérieure de Lyon, Laboratoire de Chimie Pitrat, Delphine; Ecole Normale Supérieure de Lyon, Barsu, Cyril; Lycée Carnot Andraud, Chantal; Univ Lyon, Ens de Lyon, CNRS UMR5182, Université Lyon 1, Laboratoire de Chimie. Mendonca, Cleber R.; Univ Sao Paulo, FCM Vivas, Marcelo; Universidade Federal de Alfenas, Instituto de Ciência e Tecnologia De Boni, Leonardo; Instituto de Física de São Carlos - Universidade de São Paulo, Física e Ciência dos Materiais;

Unveiling the Molecular Structure and Two-photon Absorption Properties Relationship of Branched Oligofluorenes

Leandro H. Zucolotto Cocca[a*], André Gasparotto Pelosi[a], Luis M. G. Abegão[b], Rafael de Q. Garcia, Jean-Christophe Mulatier[d], Delphine Pitrat[d], Cyrille Barsu[d],Chantal Andraud[d], Cleber R. Mendonça[a], Marcelo G. Vivas[c] and Leonardo De Boni[a,*]

[a] Photonics Group, Instituto de Física de São Carlos, Universidade de São Paulo, CP 369, 13560-970 São Carlos, SP, Brazil

[b] Grupo de Fotônica, Instituto de Física, Universidade Federal de Goiás, 74690-900, Goiânia, GO, Brazil

[c] Laboratório de Espectroscopia Ótica e Fotônica, Universidade Federal de Alfenas, 37715-400 Pocoș de Caldas, MG, Brazil

[d] ENSL, CNRS, Laboratoire de Chimie UMR 5182, 46 allée d'Italie, 69364 Lyon France

* Author to whom correspondence should be addressed: leandro.cocca@usp.br and deboni@ifsc.usp.br

Abstract

Organic molecules have been intensively studied during the last decades owing to their several photonics and biological applications. Among this material class, the fluorenes molecules present outstanding optical features, for instance, high values of two-photon absorption (2PA) cross-sections, visible transparency, and high fluorescence quantum yield. Also, it is possible to improve its nonlinear optical response by modifying its molecular structure. In this context, herein, we have synthesized V and Y-shaped branching oligofluorenes containing two and three fluorene moieties in each branch. Such a molecular strategy may exponentially enhance the nonlinear optical response due to the coherent coupling among the molecular arms. Thus, we combined the femtosecond Z-scan and white-light transient absorption spectroscopy (TAS) to understand the molecular structure and 2PA property relationship of branching oligofluorenes. The results show that there is a universal relationship between the 2PA cross-section and the effective π-electron number (N_{eff}) given by $\sigma_{2PA}\,(GM) = (0.79 \pm 0.03)\,N_{eff}^2$, which is independent of the molecular shape (linear, V or Y-shaped). Therefore, the intramolecular charge transfer responsible

for the cooperative effect among the branches does not occur. This statement is corroborated by the femtosecond TAS technique.

I – Introduction

In the last two decades, branched π-conjugated molecules have been paid much attention to observing remarkable two-photon absorption (2PA) cross-section and high optical transparency in the visible spectral window.[1-8] Together, these two features allow more efficient applications in several fields such as three-dimensional micro-fabrication, [9-12] biological imaging,[13] up-converted lasing,[14] two-photon dynamic therapy[15] and two-photon optical power limiting,[16, 17] to name a few. Therefore, several molecular designs aiming to achieve exceptional 2PA values were overwhelmed studied.[9, 10, 18-20] In this context, the best molecular strategy seems to be related to achieving the intramolecular cooperative effect, which allows maximum electronic coupling among the branches.[3, 21-25] Thus, multipolar electronic effects can arise via intramolecular charge transfer (ICT), generating, in most cases, an exponential enhancement of the 2PA cross-section as a function of the molecular shape. Other molecular designs include increasing the π-conjugation length,[26-31] adding electron-withdrawing and acceptor groups onto the π-conjugated bridge,[24, 32] modification from ortho to para or meta position groups,[33] and so on, generating only dipolar effects. These molecular strategies usually increase the 2PA cross-section quadratically with the number of π-electron.[3]

Another interesting optical feature of the branching strategy compared to the linear molecules is the possibility of increasing the nonlinear optical response while maintaining the high optical visible transparency.[23, 25, 34] This is possible because the branching effect causes a slight red-shift due to the increase of π-electron compared to the linear π-conjugated molecules. In this context, π-conjugated branched oligofluorenes are probably the most promising nonlinear optical materials due to a rigid planar biphenyl unit and large π-electron delocalization.[35, 36] Therefore, fluorene-based molecules have been studied within the nonlinear optical framework to understand the main path leading to its large 2PA cross-section. Thus, we can design new fluorene-based molecules with maximum 2PA effectiveness in order to decrease the threshold irradiance necessary to develop organic photonic devices. For example, we recently investigated the 2PA cross-section of linear oligofluorenes over the number of effective electrons (N_{eff}).[29] Herein, the primary purpose is to understand the branching effect on

the 2PA features of oligofluorenes. For that, V-shaped (V-Bis and V-Tri) and Y-shaped (Y-Bis and Y-Tri) oligofluorenes[34, 37] were investigated. Each oligofluorene has two and three fluorene moieties in each branch, as shown in Fig. 1. The 2PA spectra were collected from 460 – 800 nm employing the wavelength-tunable femtosecond Z-Scan technique. To unravel the molecular structure and 2PA properties relationship, we also studied the white-light femtosecond transient absorption spectroscopy (TAS) and the three-energy level model within the Sum-Over-State (SOS) framework.

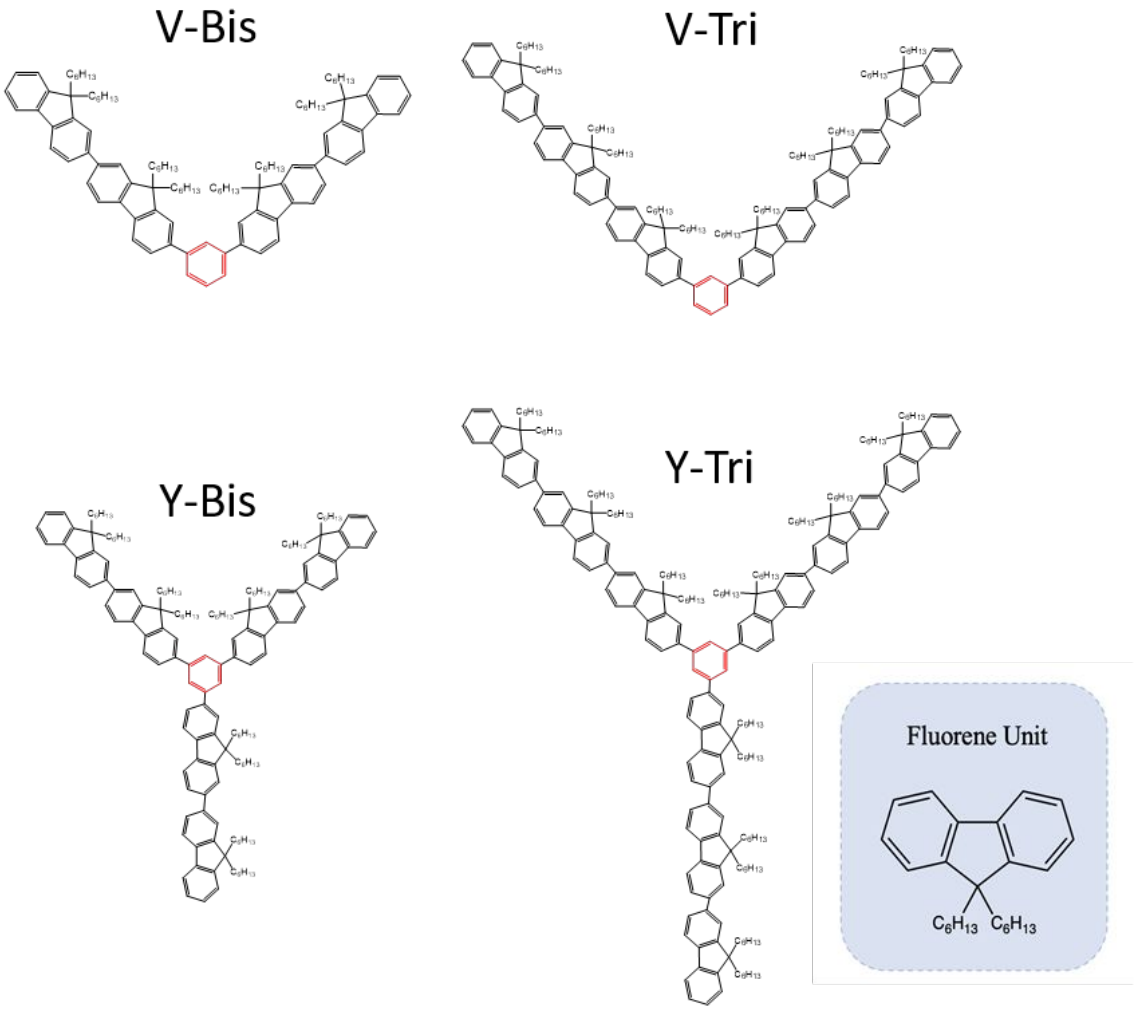

Figure 1 – Branching oligofluorenes molecular structures investigated.

II –Materials and Methods

II.1 Synthesis

The molecules synthesis is exhibited in section 1 from support information (SI).

II.2 Linear optical measurements

For linear optical measurements, the four oligofluorene molecules were dissolved in toluene in concentrations of about 10^{-6} mol/L. Fluorescence emission spectra were determined using a commercial F-7000 Hitachi fluorescence spectrophotometer and a 1 cm optical length quartz cuvette. Molar absorptivity coefficients were determined using a spectrophotometer Uv-vis Shimadzu 1800.

II.3 Femtosecond Z-scan

It was employed an optical parametric amplifier (Topas, Light Conversion) pumped by a pulse of 775 nm and 150 fs of Ti:Sapphire CPA 2001 laser system (Clark, MXR) to perform an open-aperture Z-Scan technique. Through this technique, we were able to determine the 2PA cross-section spectra, for the four oligofluorenes, in a spectral range from 460 nm to 800 nm. Details on the experimental setup can be found in Ref. 29. It is important to mention that we employed this technique owing to the ease and quickness of performing 2PA measurements. Moreover, data acquisition and analysis of results of that technique are performed quickly and substantially accurately, allowing us to obtain 2PA cross sections with experimental errors of around 10-15%.

II.4 Femtosecond white-light Transient absorption

The same laser system used in the Z-scan technique was employed for the femtosecond white-light transient absorption. The pump (387.5 nm) and probe (white-light continuum) beams were obtained from a second-harmonic generation crystal (BBO) and a sapphire window (1 mm of thickness), respectively. A resolution of ~187.5 fs is obtained, controlling the delay between pump and probe pulses through the high-resolution translation stage. The time-resolved transient absorption spectra (ΔA) were monitored using a fast spectrometer. To avoid photobleaching, we used pump pulses with energy smaller than 1 μJ. Details on the experimental setup can be found in Refs. [38, 39].

III – Results and discussion

All samples present one electronic band ($S_0 \rightarrow S_1$, $1A_g$-like $\rightarrow$ $1B_u$-like) in the UV region (300 – 400 nm), as shown in Fig. 2. The molar absorptivity (ε) bands are

spectrally located at 344 nm, 359 nm, 347 nm, and 360 nm for V-Bis, V-Tri, Y-Bis, and Y-Tri, respectively, with values between 2.0 and $3.3 \times 10^5\, L\, cm^{-1}\, mol^{-1}$. As one can notice, the molecules with two fluorene moieties (V-Bis and Y-Bis) have a molar absorptivity band around 350 nm. In comparison, the molar absorptivity bands of molecules with three fluorene moieties (V-Tri and Y-Tri) are located around 360 nm. V- or Y-shaped molecules bearing the same number of fluorenes moieties present a similar absorption wavelength, while the introduction of a fluorene on each branch induces a 10 nm absorption red-shift. Regarding molar absorptivity ratio values, it is noted that there is an increase of 1.25 for the V-shaped samples, or in other words, $\frac{\varepsilon_{Vtri}}{\varepsilon_{Vbis}} = 1.25$. In the same way, there is an increase of 1.47 regarding the Y-shaped molecules, $\frac{\varepsilon_{Ytri}}{\varepsilon_{Ybis}} = 1.47$. These results show that there is a very similar increase rate ε values when passing from Bis to Tris molecules, in the case of V or Y shaped molecules. Also, $\frac{\varepsilon_{Ybis}}{\varepsilon_{Vbis}} = 1.10$ and $\frac{\varepsilon_{Ytri}}{\varepsilon_{Vtri}} = 1.28$, showing the same when passing from V to Y molecules, in the case of Bis or Tri. In this way, it may be helpful to analyze the linear and nonlinear optical properties as a function of the increase of π-electrons. So, using the concept of the effective number of electrons[40] ($N_{eff} = \sqrt{\sum n_i^2}$, in which n is the number of π-electrons), we can find out how the variation of optical properties is as a function of the N_{eff}.

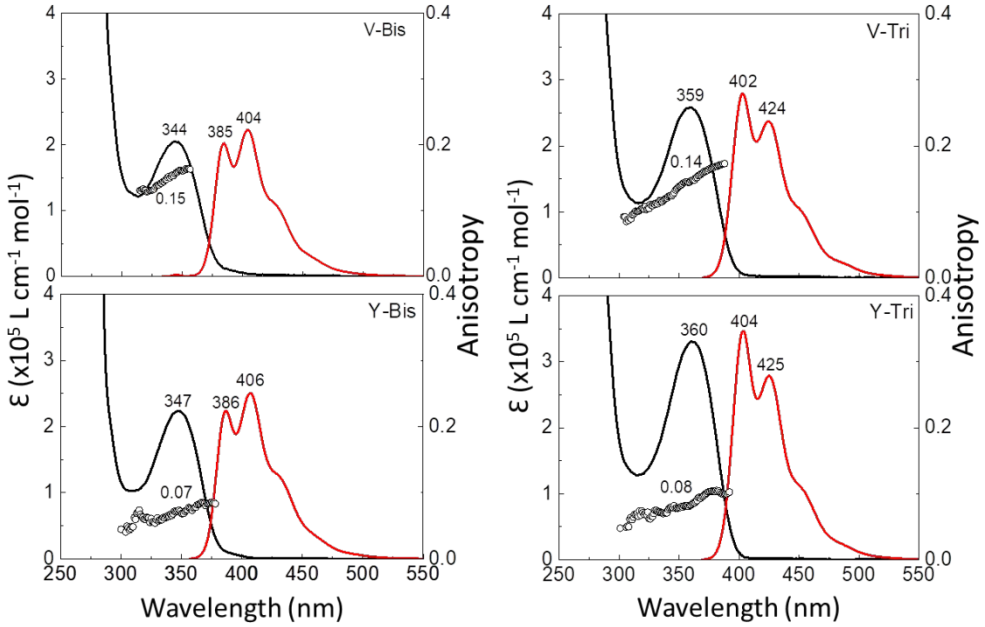

Figure 2: One-photon absorption spectra (left axis – black lines), anisotropy (black circles, right-axis) factor r, and normalized fluorescence emission (red lines) for Y and V-shaped oligofluorenes.

According to Ref.[40], one can calculate the N_{eff} and it was observed the following results: $N_{eff}^{VBis} = \sqrt{4x12^2 + 6^2} \cong 25$, $N_{eff}^{VTri} = \sqrt{6x12^2 + 6^2} \cong 30$, $N_{eff}^{YBis} = \sqrt{6x12^2 + 6^2} \cong 30$ and $N_{eff}^{YTri} = \sqrt{9x12^2 + 6^2} \cong 37$. Considering the molar absorptivity peak values (Table 1), we can observe that $\frac{\varepsilon_{Vbis}}{N_{eff}^{VBis}} = 8.8 \times 10^3\, L\, cm^{-1}\, mol^{-1}$, $\frac{\varepsilon_{Vtri}}{N_{eff}^{VTri}} = 8.6 \times 10^3\, L\, cm^{-1}\, mol^{-1}$, $\frac{\varepsilon_{Ybis}}{N_{eff}^{YBis}} = 7.5 \times 10^3\, L\, cm^{-1}\, mol^{-1}$and $\frac{\varepsilon_{YTri}}{N_{eff}^{YTri}} = 9.0 \times 10^3\, L\, cm^{-1}\, mol^{-1}$, so, there is a contribution about $9.0 \times 10^3\, L\, cm^{-1}\, mol^{-1}$ per N_{eff}.

The fluorescence emission, for all molecules, occurs at the UV-Vis region in a range from 360 – 520 nm, with a maximum of around 400 – 425 nm according to each molecule. The fluorescence quantum yield (ϕ) for all compounds dissolved in toluene was determined and results revealed that Y-Tri and V-Tri presented values of 14% and 18%, respectively, as well Y-Bis and V-Bis presented values of 25% and 43%, respectively. The increase in ϕ values of Bis-shaped could be understood owing to its more rigid structure supporting the radiative decays. More details about fluorescence quantum yield measurements can be seen in the Supporting Information. The Y-bis and Y-tris oligofluorenes fluorescence lifetimes (τ_f) can be found in Refs. [34, 37], while the time-resolved fluorescence curves for the V-Bis and V-Tri are in Supporting information. Table 1 depicts the fluorescence lifetime values for all oligofluorenes.

The splitting of the lowest-energy state, expected in these branched molecules,[41] is confirmed by the fluorescence anisotropy spectra (Fig. 2 – black circles) determined using the following equation:[42]

$$r(\lambda) = \frac{I_{vv} - GI_{vh}}{I_{vv} + 2GI_{vh}} \quad (1)$$

in which I is the fluorescence excitation intensity spectra and G is the experimental factor related to channels (excitation and emission) sensibility. The subscribed vv, vh, hv, and hh are the polarization excitation and emission channels with v = vertical and h = horizontal. It is important to highlight that, to determine $r(\lambda)$, the emission wavelength was fixed at around 430 nm, and the excitation wavelengths ranged from 290 – 400 nm. It is observed that the anisotropy spectra present a continuous change in a spectral range from 300 to 400 nm. Moreover, the anisotropy values shown inset of Figure 2

correspond to the ε maxima of each compound. Thus, we calculated the transition dipole moment from the ground to the first excited state ($1A_g$-like → $1B_u$-like) using:

$$\mu_{1A_g \rightarrow 1B_u} = \sqrt{\frac{3 \times 10^3 \ln(10)\, hc\, n}{8\pi^3} \frac{1}{N_A L^2 \omega_{1A_g \rightarrow 1B_u}} \int \varepsilon(\omega) d\omega} \quad (2)$$

in this equation, $\omega_{1A_g \rightarrow 1B_u}$ represents the transition frequency from the ground to first excited state $1A_g$-like → $1B_u$-like. Also, h, c, n, N_A, ω, L, and $\int \varepsilon(\omega) d\omega$ are Planck constant, speed of light, solvent refractive index (toluene), Avogadro constant, photon frequency, Onsager local field factor ($L = \frac{3n^2}{2n^2+1}$) and molar absorption area, respectively. In view of determine $\int \varepsilon(\omega) d\omega$, was performed Gaussians decomposition (see Figure SI1 from Support Information). The values of $\mu_{1A_g \rightarrow 1B_u}$, for each molecule, are presented in Table 1. Looking at $\mu_{1A_g \rightarrow 1B_u}$ values, it is possible to see that: $\frac{\mu_{V_{Tri}}}{\mu_{V_{Bis}}} = 1.21$ and $\frac{\mu_{Y_{Tri}}}{\mu_{Y_{Bis}}} = 1.26$, so, $\mu_{1A_g \rightarrow 1B_u}$ increases in the same rate for V and Y-shaped oligofluorenes molecules, indicating that this spectroscopic parameter seems to be independent of molecular structure shape, as pointed out by the molar absorptivity results. It was also determined the $\mu_{1A_g \rightarrow 1B_u}$ rate, according to the N_{eff} of each molecule, the results show that there is a contribution of about 0.5 D per N_{eff} for all molecules: $\frac{\mu_{1A_g \rightarrow 1B_u}^{V_{Bis}}}{N_{eff}^{V_{Bis}}} = \frac{13.5\ D}{24.73} = 0.54$ D, $\frac{\mu_{1A_g \rightarrow 1B_u}^{V_{Tri}}}{N_{eff}^{V_{Tri}}} = \frac{16.4\ D}{30} = 0.54$ D, $\frac{\mu_{1A_g \rightarrow 1B_u}^{Y_{Bis}}}{N_{eff}^{Y_{Bis}}} = \frac{15\ D}{30} = 0.50$ D, $\frac{\mu_{1A_g \rightarrow 1B_u}^{Y_{Tri}}}{N_{eff}^{Y_{Tri}}} = \frac{18.9\ D}{36.49} = 0.51$ D. Thus, the $\mu_{1A_g \rightarrow 1B_u}$ of oligofluorenes follows a linear relationship with N_{eff}, which is the same relationship found for linear oligofluorenes.[29]

Table 1: Linear optical properties of studied branched oligofluorenes. Molar absorptivity (ε), fluorescence lifetime (τ_f), anisotropy (r) and $\mu_{1A_g \rightarrow 1B_u}(D)$ is the transition dipole moment ($1A_g$-like → $1B_u$-like).

	$\varepsilon(10^5 L cm^{-1} mol^{-1})$	τ_f (ps)	r (ε maxima)	$\mu_{1A_g \rightarrow 1B_u}(D)$
V-Bis	2.0	700 ± 100	0.15 ± 0.05	14 ± 1
V-Tri	2.6	700 ± 100	0.14 ± 0.04	16 ± 2
Y-Bis	2.2	500[34]	0.07 ± 0.02	15 ± 2

Y-Tri	3.3	350[34]	0.08 ± 0.02	19 ± 2

Figure 3 depicts the 2PA spectra (see SI) for all molecules obtained through the wavelength-tunable femtosecond Z-scan technique. All samples present one intense 2PA band in the visible region, which is attributed to the pure 2PA transition in fluorenes ($1A_g$-like $\rightarrow 2A_g$-like). Such electronic transition for both V-Tri and Y-Tri fluorenes exhibit 2PA peaks in higher wavelengths (around 600 nm) than V-Bis and Y-Bis oligofluorenes, whose 2PA peaks are located around 580 nm. This feature may be explained by the increase in the π-conjugation length in Tri fluorenes. The σ_{2PA} peak values are for V-Bis (578 GM), V-Tri (721 GM), Y-Bis (612 GM), and Y-Tri (1018 GM). For the same branch length, Y shape molecules present higher σ_{2PA} values. We have also observed a weak 2PA band (20-50 GM) in the 700 – 800 nm spectral region. This 2PA band is located in the same spectral region as the lowest-energy 1PA-allowed band. As the fluorene molecule has a plane symmetry (symmetry point group C_{2v}),[43] but does not present an inversion center, the 1PA allowed transition is weakly 2PA allowed.[44]

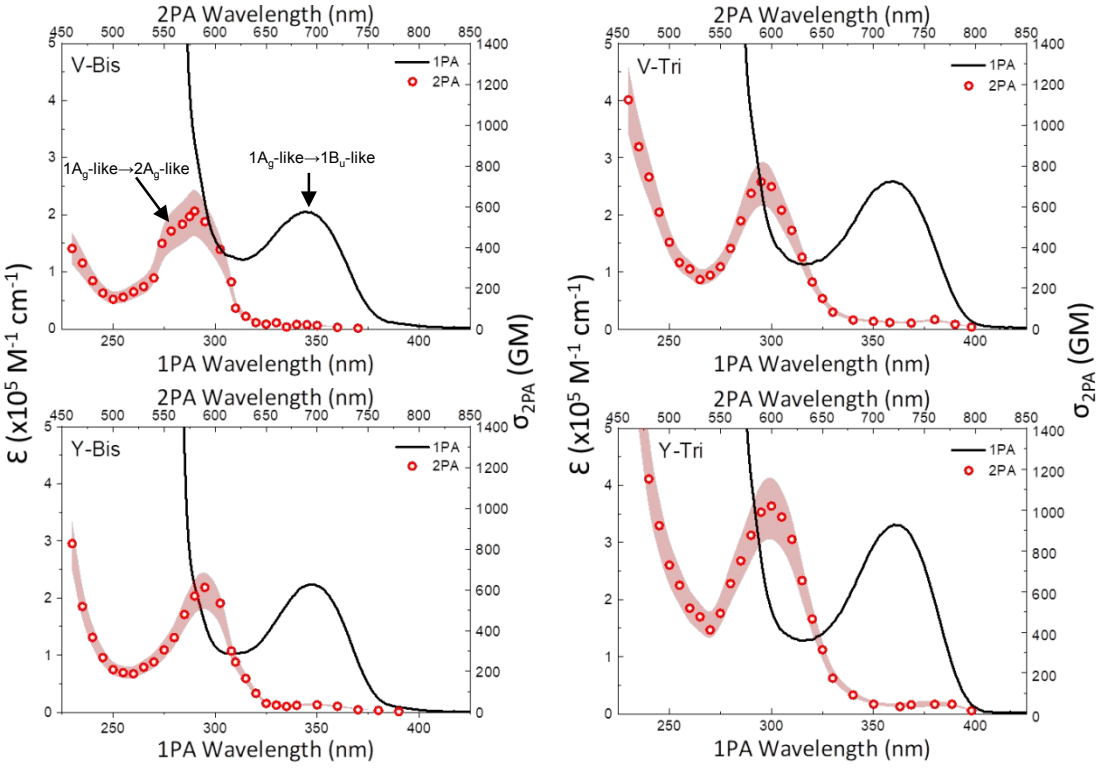

Figure 3: 1PA spectra (black lines), 2PA cross-section (circles) for Y and V-shaped oligofluorenes. The shadow on the 2PA data corresponds to the standard deviation. The Z-Scan fittings are exhibited in Figure SI2 from support information.

The intermediate state resonance enhancement (ISRE) effect also was observed in the 2PA transitions for wavelengths lower than 520 nm. Such an effect is very pronounced as the excitation photon energy approaches the lowest-energy 1PA-allowed transition, which can lead to the 2PA double resonance.[38] Also, the high excited-state absorption greatly influences this effect.[45]

Regarding the pure 2PA band ($1A_g$-like→$2A_g$-like), in Fig.4, we show the 2PA cross-section peak as a function of N_{eff} for the linear (Tri, Penta, Hepta)[29] and branching (V-Bis, V-Tri, Y-Bis, and Y-Tri) oligofluorenes. The solid and dashed lines in Fig. 4 illustrate the quadratic and linear fitting used to model the nonlinear optical response. It is worth mentioning that we have put to zero the first and second-order coefficients in both fittings because the $N_{eff} = 0$ implies necessarily $\sigma_{2PA} = 0$. As can be seen, the best fitting was the quadratic function described by $\sigma_{2PA}\,(GM) = (0.79 \pm 0.03)N_{eff}^2$. Such behavior is characteristic of the organic structures with a strong dipolar character and a high degree of molecular symmetry. [3, 24] In general, in such a molecular system, the transition dipole moment is proportional to the square root of the N_{eff}.[40] Thus, the 2PA cross section can be described approximately for the three-energy level system within the sum-over-states framework for centrosymmetric molecules.[46] The inset in Fig. 4 illustrates the three-energy level system emphasizing the main energy levels involved in the 2PA-induced transitions in oligofluorenes. In this context, σ_{2PA} is proportional to the fourth power of the transition dipole moment. Consequently, a quadratic dependency is obtained between the 2PA cross section and the N_{eff}. Therefore, these outcomes show that the 2PA cross-section for the $1A_g$-like→$2A_g$-like transition in oligofluorenes is independent of the molecular shape (linear, V, or Y).

To deeper understand such an interesting outcome, we performed the white-light femtosecond TAS. As mentioned, the electronic cooperative effect among the branches rises via intramolecular charge transfer (ICT) in branching molecules. The white-light femtosecond TAS is a powerful technique to probe the ultrafast dynamics such as ICT.[2, 47, 48] Figure 5 (a) illustrates TAS colormap representing time- and wavelength-resolved dynamics. The results show an excited-state absorption (ESA, $\Delta A > 0$) band located at ~705 nm for V-Bis and Y-Bis, while for V-Tris and Y-Tris the ESA band rises at ~750 nm. This strong ESA ($\omega_{pump} + \omega_{probe}$), observed by ultrafast TA, does not contribute to the 2PA band located at *c.a.* 600 nm. Alternatively, it corresponds to the enhancement effect region for wavelengths shorter than 520 nm.

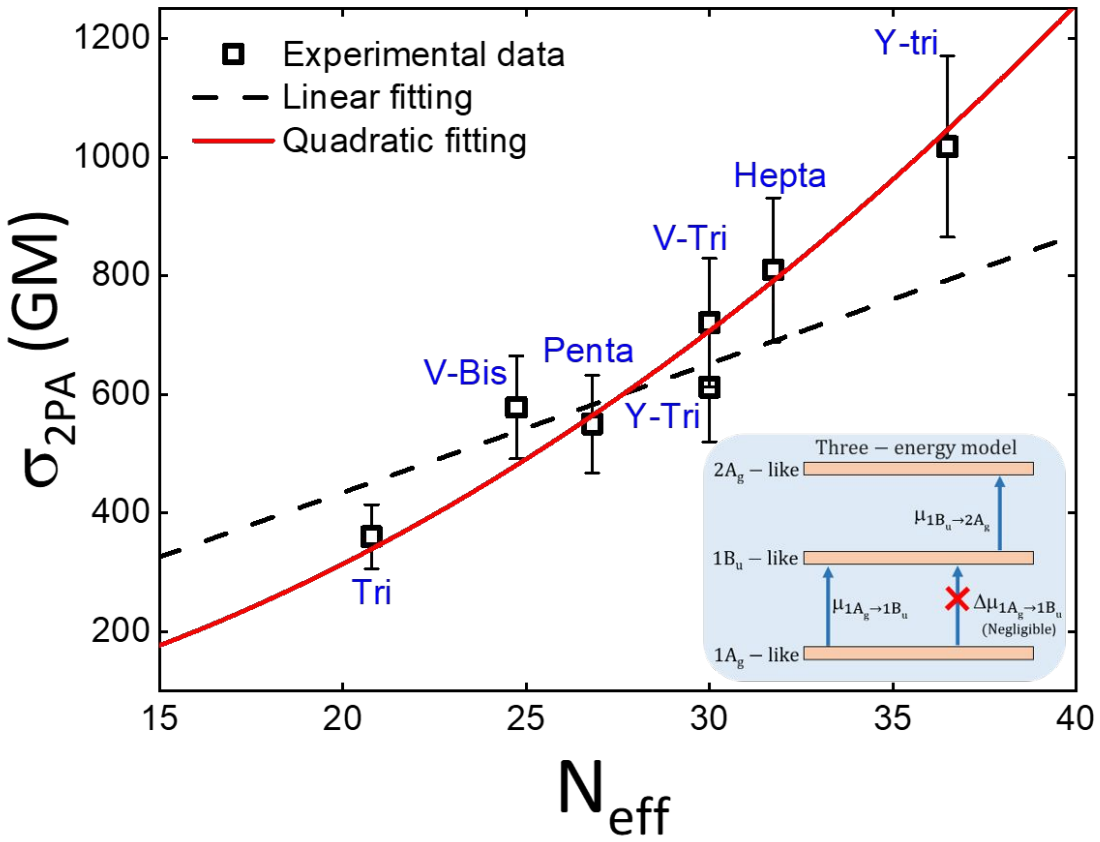

Figure 4: Relation between the 2PA cross-section and N_{eff} for linear (Tri, Penta, and Heptafluorene) and branching (V-bis, V-Tris, Y-Bis, and Y-Tris) oligofluorenes. The inset shows the three-energy model employed to perform SOS analysis.

Concerning the temporal dynamics, as shown in Figure 5 and in Supporting Information, the branching oligofluorenes did not present an ultrafast dynamic characteristic time of the coherent coupling among the branches (cooperative effect). ICT is generally responsible for the cooperative effect in branching molecules occurring in a timescale between 1 and 10 ps. As shown in SI, the time-domain TAS signal remains virtually constant during all delay times (~10 ps).[2] Global Analysis of the data revealed that an instrument response function of ~ 1 ps FWHM convoluted with one exponential decay equal to the fluorescence lifetime (300 – 700 ps) is sufficient for explaining the TAS signal. Our outcomes thus show that this is the only dynamic related to the branching oligofluorenes. Therefore, the branching effect poorly influences the cross-section of the pure 2PA transition in oligofluorenes.

As shown, the branching molecules present a dipolar character analogous to the linear oligofluorenes. In this case, we can shade more light on the 2PA properties and employ the three-energy model within the SOS approach to obtain information about

the excited states for the branching oligofluorenes. Thus, $1B_u$-like →$2A_g$-like transition dipole moment, $|\vec{\mu}_{1B_u \to 2A_g}|$, can be obtained directly from the pure 2PA transition located at 600 nm as follows:[3,24,38,46]

$$|\vec{\mu}_{1B_u \to 2A_g}|^2 = \frac{5(nhc)^2}{2\,(2\pi)^5\, L^4 R(\omega,\omega_{1A_g \to 1B_u})\, |\vec{\mu}_{1A_g \to 1B_u}|^2} \sqrt{\frac{\pi \Gamma^2_{1A_g \to 2A_g}}{4\log(2)}} \sigma^{(2PA)}_{1A_g \to 2A_g} \qquad (3)$$

in which $|\vec{\mu}_{1A_g \to 1B_u}|$ is the transition dipole moment between the ground and the first excited states ($1A_g$-like → $1B_u$-like), $\sigma^{(2PA)}_{1A_g \to 2A_g}$ is the 2PA cross-section related to $1A_g$-like → $2A_g$-like pure transition and $R(\omega,\omega_{1A_g \to 1B_u}) = \omega^2 / \left[(\omega_{1A_g \to 1B_u} - \omega)^2 + \Gamma^2_{1A_g \to 1B_u}\right]$ is the resonance enhancement factor. $\Gamma_{1A_g \to 1B_u}$ and $\Gamma_{1A_g \to 2A_g}$ are the full width at half maximum referred to the $1A_g$-like → $1B_u$-like (1PA allowed) and $1A_g$-like → $2A_g$-like (2PA allowed) transitions, both obtained from Figure 3, considering a Gaussian line-shaped for both 1PA and 2PA spectra.

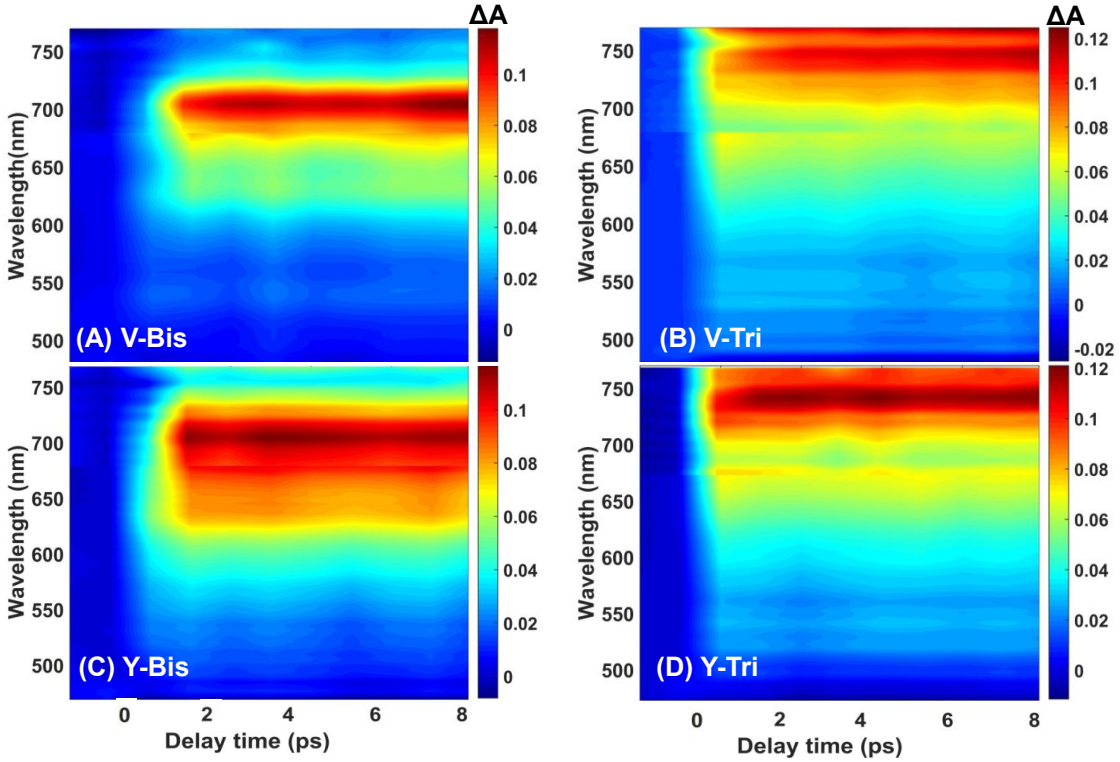

Figure 5: Transient absorptions measurements for V and Y-shaped oligofluorenes.

Figure 6 illustrates the ground and excited-state dipole transition moment relationship for the linear and branching oligofluorenes. As noted, a constant value for

the ESA dipole moment is noticed for the branching molecules. Contrariwise, ESA intensity reduces as a function of the increase of fluorene moieties for linear oligofluorenes. These results indicate that a higher conformational disorder is induced in linear oligofluorenes, most probably, because of their larger conjugation length.[49] This spurious effect seems to be fixed through the branching mechanism. Nevertheless, the ESA dipole moment for the branching is smaller than linear oligofluorenes due to the absence of coherent coupling among the branches, as pointed out in the TAS.

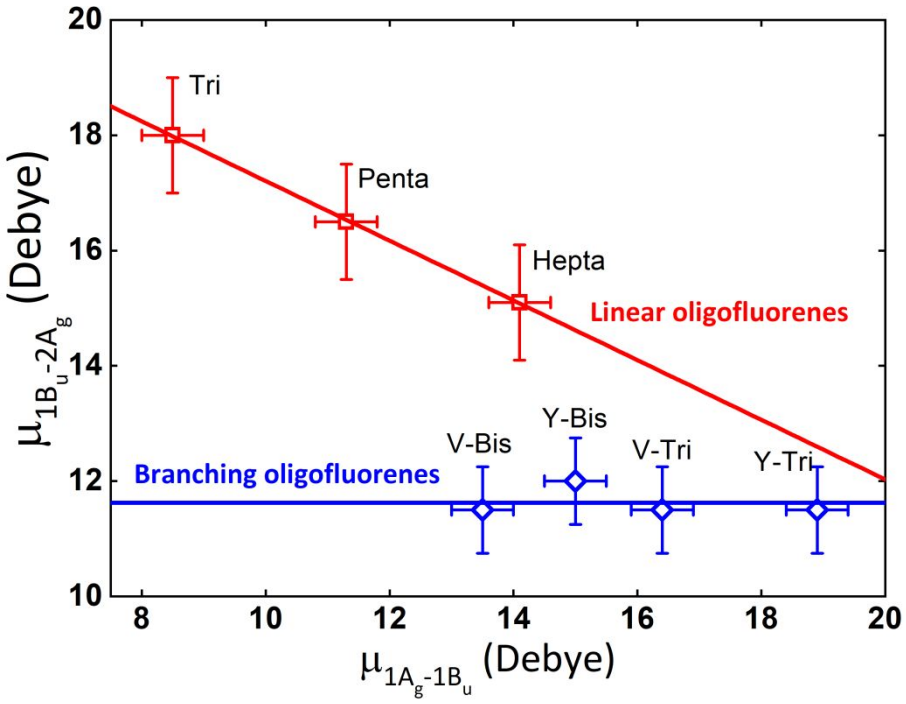

Figure 6 – Comparison between the ground and excited-state transition dipole moment for the linear and branching oligofluorenes. All values were obtained using the SOS approach.

IV – FINAL REMARKS

Herein, we carefully studied the molecular structure and 2PA property relationship of branching oligofluorenes. We found a universal relation between the 2PA cross-section and N_{eff}, which follows a quadratic dependence described by $\sigma_{2PA}(GM) = (0.79 \pm 0.03)N_{eff}^2$. These results show that the V and Y-shaped oligofluorenes have a dipolar character analogous to the linear oligofluorenes. Through the TAS measurements, we reported that the coherent coupling among the branches, which can enhance the 2PA, is not observed in these structures. All branching molecules present a benzene core, which may act as an electron-withdrawing or acceptor group, depending on the attached group. In our case, we have the fluorene molecule that acts as a π-conjugated bridge or can introduce a weak electron-accepting

character. Thus, $(A-\pi-A)_2$ or $(A-\pi-A)_3$ structures can be formed, but they do not generate a push-pull configuration that is vital to generating a robust cooperative effect.

Supporting Information

Support information includes the experimental results of absorption bands Gaussian decompositions, Femtosecond transient absorption, time-resolved fluorescence measurements, fluorescence quantum yields measurements, and Z-scan fittings.

Acknowledgments

Financial support from FAPESP (Fundação de Amparo à Pesquisa do Estado de São Paulo, grants 2016/20886-1, 2018/11283-7, 2020/16036-8 and 2022/06561-3), FAPEMIG (Fundação de Amparo à Pesquisa do Estado de Minas Gerais, grant APQ-01469-18), CNPq (Conselho Nacional de Desenvolvimento Científico e Tecnológico, grant 425180/2018-2), Coordenação de Aperfeiçoamento de Pessoal de Nível Superior (CAPES) Finance Code 001, Army Research Laboratory (W911NF-17-1-0123) and Air Force Office of Scientific Research (FA9550-12-1-0028) are acknowledged.

References

1. N. Ripoche *et al.*, Physical Chemistry Chemical Physics, 2021, **23**, 22283-22297.
2. F. Kournoutas *et al.*, Physical Chemistry Chemical Physics, 2020, **22**, 4165-4176.
3. R. D. Fonseca, M. G. Vivas, D. L. Silva, G. Eucat, Y. Bretonniere, C. Andraud, C. R. Mendonca, and L. De Boni, Journal of Physical Chemistry Letters, 2019, **10**, 2214-2219.
4. X. Zhou, A. M. Ren, J. K. Feng, X. J. Liu, J. X. Zhang, and J. Z. Liu, Physical Chemistry Chemical Physics, 2002, **4**, 4346-4352.
5. L. Porres, O. Mongin, C. Katan, M. Charlot, B. K. C. Bhatthula, V. Jouikov, T. Pons, J. Mertz, and M. Blanchard-Desce, Journal of Nonlinear Optical Physics & Materials, 2004, **13**, 451-460.
6. F. S. Meng, J. Mi, S. X. Qian, K. C. Chen, and H. Tian, Polymer, 2003, **44**, 6851-6855.
7. P. Macak, Y. Luo, P. Norman, and H. Agren, Journal of Chemical Physics, 2000, **113**, 7055-7061.
8. I. Fuks-Janczarek *et al.*, Optics Communications, 2002, **209**, 461-466.
9. B. H. Cumpston *et al.*, Nature, 1999, **398**, 51-54.
10. S. Kawata, H. B. Sun, T. Tanaka, and K. Takada, Nature, 2001, **412**, 697-698.
11. S. Maruo, and K. Ikuta, in *Conference on Micro- and Nano-photonic Materials and Devices*San Jose, Ca, 2000), pp. 106-112.
12. S. Maruo, O. Nakamura, and S. Kawata, Optics Letters, 1997, **22**, 132-134.

13. W. Denk, Proceedings of the National Academy of Sciences of the United States of America, 1994, **91**, 6629-6633.
14. A. Mukherjee, Applied Physics Letters, 1993, **62**, 3423-3425.
15. T. T. Zhao *et al.*, Acs Applied Materials & Interfaces, 2014, **6**, 2700-2708.
16. Y. Morel, A. Irimia, P. Najechalski, Y. Kervella, O. Stephan, P. L. Baldeck, and C. Andraud, Journal of Chemical Physics, 2001, **114**, 5391-5396.
17. P. Poornesh, P. K. Hegde, G. Umesh, M. G. Manjunatha, K. B. Manjunatha, and A. V. Adhikari, Optics and Laser Technology, 2010, **42**, 230-236.
18. K. D. Belfield, M. V. Bondar, A. R. Morales, X. L. Yue, G. Luchita, and O. V. Przhonska, Journal of Physical Chemistry C, 2012, **116**, 11261-11271.
19. M. Drobizhev, N. S. Makarov, A. Rebane, G. de la Torre, and T. Torres, Journal of Physical Chemistry C, 2008, **112**, 848-859.
20. R. Fortrie, R. Anemian, O. Stephan, J. C. Mulatier, P. L. Baldeck, C. Andraud, and H. Chermette, Journal of Physical Chemistry C, 2007, **111**, 2270-2279.
21. E. Collini, Physical Chemistry Chemical Physics, 2012, **14**, 3725-3736.
22. L. Zhao, G. C. Yang, Z. M. Su, and L. K. Yan, Journal of Molecular Structure-Theochem, 2008, **855**, 69-76.
23. M. Drobizhev, A. Karotki, Y. Dzenis, M. Kruk, A. Rebane, Z. Suo, and C. W. Spangler, in *Conference on Nonlinear Optical Transmission and Multiphoton Processes in Organics*San Diego, Ca, 2003), pp. 38-47.
24. A. Rebane, M. Drobizhev, N. S. Makarov, E. Beuerman, J. E. Haley, M. K. Douglas, A. R. Burke, J. L. Flikkema, and T. M. Cooper, Journal of Physical Chemistry A, 2011, **115**, 4255-4262.
25. M. Drobizhev, A. Karotki, Y. Dzenis, A. Rebane, Z. Y. Suo, and C. W. Spangler, Journal of Physical Chemistry B, 2003, **107**, 7540-7543.
26. I. Cohanoschi, K. D. Belfield, C. Toro, S. Yao, and F. E. Hernandez, Journal of Chemical Physics, 2006, **124**.
27. O. Rubio-Pons, Y. Luo, and H. Agren, Journal of Chemical Physics, 2006, **124**.
28. M. G. Vivas, and C. R. Mendonca, Journal of Physical Chemistry A, 2012, **116**, 7033-7038.
29. L. M. G. Abegao, L. H. Z. Cocca, J. C. Mulatier, D. Pitrat, C. Andraud, L. Misoguti, C. R. Mendonca, M. G. Vivas, and L. De Boni, Physical Chemistry Chemical Physics, 2021, **23**, 18602-18609.
30. J. D. Bhawalkar, G. S. He, and P. N. Prasad, Reports on Progress in Physics, 1996, **59**, 1041-1070.
31. S. L. Oliveira, D. S. Correa, L. De Boni, L. Misoguti, S. C. Zilio, and C. R. Mendonca, Applied Physics Letters, 2006, **88**.
32. M. G. Vivas *et al.*, Scientific Reports, 2014, **4**.
33. B. Osmialowski *et al.*, Journal of Physical Chemistry Letters, 2020, **11**, 5920-5925.
34. C. Barsu, C. Andraud, N. Amari, S. Spagnoli, and P. L. Baldeck, Journal of Nonlinear Optical Physics & Materials, 2005, **14**, 311-318.
35. X. Zhou, J. K. Feng, and A. M. Ren, Chemical Physics Letters, 2004, **397**, 500-509.
36. R. Anemian, J. C. Mulatier, C. Andraud, Y. Morel, O. Stephan, and P. L. Baldeck, in *Conference on Multiphoton Absorption and Nonlinear Transmission Processes - Materials, Theory and Applications*Seattle, Wa, 2002), pp. 25-32.
37. C. Barsu, R. Anemian, C. Andraud, O. Stephan, and P. L. Baldeck, Molecular Crystals and Liquid Crystals, 2006, **446**, 175-182.

38. M. G. Vivas, L. De Boni, T. M. Cooper, and C. R. Mendonca, Acs Photonics, 2014, **1**, 106-113.
39. M. G. Vivas, J. P. Siqueira, D. L. Silva, L. de Bonia, and C. R. Mendonca, Rsc Advances, 2015, **5**, 74531-74538.
40. M. G. Kuzyk, Journal of Chemical Physics, 2003, **119**, 8327-8334.
41. N. S. Makarov, S. Mukhopadhyay, K. Yesudas, J. L. Bredas, J. W. Perry, A. Pron, M. Kivala, and K. Mullen, Journal of Physical Chemistry A, 2012, **116**, 3781-3793.
42. J. R. Lakowicz, *Principles of Fluorescence Spectroscopy* (Springer, 2006),
43. S. Chakrabortya, P. Das, S. Manogaranb, and P. K. Das, Vibrational Spectroscopy, 2013, **68**, 162-169.
44. S. Zein, F. Delbecq, and D. Simonb, Physical Chemistry Chemical Physics, 2008, **11**, 694–702.
45. J. M. Hales *et al.*, Journal of Chemical Physics, 2004, **121**, 3152-3160.
46. M. G. Vivas, L. De Boni, and C. R. Mendonca, in *Molecular and Laser Spectroscopy*, edited by V. P. Gupta (Elsevier, 2018).
47. S. E. Canton *et al.*, Nature Communications, 2015, **6**.
48. Y. G. Yang, Y. Liu, B. D. Feng, H. Zhang, C. C. Qin, K. Yu, K. Jiang, and Y. F. Liu, Journal of Luminescence, 2022, **242**.
49. M. L. Raicoski, and M. G. Vivas, Journal of Physical Chemistry B, 2021, **125**, 9887-9894.